Article

Discovery Medicine 2026; 38(214): 3490–3503
https://doi.org/10.24976/Discov.Med.202638214.267

FASN Involvement in the Protective Effects of Aloe Emodin Against LPS-induced Pulmonary Microvascular Endothelial Cell Injury

Shiping Zhu[1], Haoran Deng[1], Xuchun Ding[1], Lihong Zhu[1,*], Zhijun Li[1,*]

[1]Department of Respiratory and Critical Care Medicine, Hangzhou Hospital of Traditional Chinese Medicine, 310007 Hangzhou, Zhejiang, China
*Correspondence: zhulihong_hztcm@163.com (Lihong Zhu); lzj13575748493@sina.com (Zhijun Li)
Submitted: 17 July 2026 Revised: 25 August 2026 Accepted: 4 September 2026 Published: 25 November 2026

Background: Pulmonary microvascular endothelial cells (PMVECs) are implicated in maintaining alveolar barrier integrity, and endothelial injury is a key event in the pathogenesis of pneumonia. Rhubarb exhibits anti-inflammatory and endothelial protective properties, but its active components and mechanisms of action in pneumonia remain unclear.

Methods: Network pharmacology analysis was performed to elucidate the mechanism of rhubarb against pneumonia. The interaction between Aloe emodin (AE) and its potential target was predicted by molecular docking. An *in vitro* model of lipopolysaccharide (LPS)-stimulated human PMVECs (HPMVECs) was treated with AE (20 µmol/L or 40 µmol/L), or AE combined with a fatty acid synthase (FASN) overexpression plasmid. Cellular injury, inflammation, lipid metabolism, and key lipogenic genes were assessed using cell viability assays, apoptosis detection, enzyme-linked immunosorbent assay (ELISA), Nile Red staining, and quantitative real-time PCR (qRT-PCR).

Results: AE and FASN exhibited a stable binding pattern, as indicated by molecular docking. In LPS-stimulated HPMVECs, AE significantly improved cell viability, reduced apoptosis, downregulated pro-inflammatory cytokines interleukin-6 (IL-6) and tumor necrosis factor-alpha (TNF-α), and alleviated lipid droplet accumulation ($p < 0.05$). AE also reversed LPS-induced lipid metabolism disorders by restoring free fatty acid, cholesterol, and triglyceride levels, and suppressing the mRNA expression of lipogenic genes sterol regulatory element binding transcription factor 1 (*SREBF1*), ATP citrate lyase (*ACLY*), stearoyl-CoA desaturase (*SCD1*), *FASN*, and 3-hydroxy-3-methylglutaryl-CoA reductase (*HMGCR*) ($p < 0.05$). Crucially, the protective effects of AE were attenuated by FASN overexpression ($p < 0.05$).

Conclusion: AE exhibits broad protective actions against LPS-induced HPMVEC injury by ameliorating inflammation and lipid metabolism disorders, potentially through FASN regulation. Our findings provide new empirical evidence supporting the potential utility of rhubarb-derived compounds in alleviating LPS-induced endothelial cell injury.

Keywords: pneumonia; AE; *FASN*; lipid metabolism; PMVECs; network pharmacology

Introduction

Pneumonia is a common and severe pulmonary infectious disease; its progression may lead to acute lung injury (ALI) and even acute respiratory distress syndrome (ARDS), culminating in hypoxemic respiratory failure and posing a significant threat to patient survival [1]. Despite decades of intensive research, effective pharmacotherapies remain elusive, and clinical management still relies largely on supportive care [2]. Therefore, developing novel therapeutic interventions that directly target the underlying pathophysiological mechanisms of pneumonia remains an urgent clinical priority.

Pulmonary microvascular endothelial cells (PMVECs) play a pivotal role in maintaining lung homeostasis, and their dysfunction—characterized by excessive apoptosis, inflammatory activation, and metabolic disturbances—is considered a critical event in the pathogenesis of pneumonia [3]. Therefore, protecting PMVECs from injury, suppressing excessive inflammatory responses, and correcting metabolic dysregulation represent viable therapeutic strategy for pneumonia.

Emerging metabolomic and transcriptomic evidence have revealed that metabolic reprogramming, particularly lipid metabolic dysregulation, is a key factor in endothelial injury during pneumonia [4]. Fatty acid synthase (FASN), a key enzyme responsible for the terminal reaction of *de novo* fatty acid synthesis, has gained attention as a plausible therapeutic target in ALI [5]. Inhibition of FASN has been shown to alleviate ALI and endothelial dysfunction [6], highlighting the significance of FASN-mediated fatty acid metabolism in the pathogenesis of pneumonia.

Rhubarb (Dahuang) is a medicinal plant rich in bioactive anthraquinones. Modern pharmacological studies have demonstrated that rhubarb and its major active constituents can regulate glucose and lipid metabolism [7,8].

Copyright: © 2026 The Author(s). Published by Discovery Medicine. This is an open access article under the CC BY 4.0 license.
Note: *Discovery Medicine* stays neutral with regard to jurisdictional claims in published maps and institutional affiliations.

Among the bioactive compounds derived from rhubarb, aloe emodin (AE) has attracted increasing attention. The roots and rhizomes of Rheum palmatum L. serve as a natural source of AE, an anthraquinone derivative [9]. Recent studies have revealed that AE exhibits significant anti-inflammatory properties and protects against endothelial junction dysfunction [10]. However, whether AE exerts protective effects on PMVECs under pneumonia conditions, and whether such protection is associated with the regulation of FASN-driven fatty acid metabolism, remain largely unexplored.

In the present study, we used lipopolysaccharide (LPS)-stimulated human PMVECs (HPMVECs) as an *in vitro* model to mimic pneumonia-associated endothelial injury. Here, we investigated whether AE protects HPMVECs from LPS-induced injury and metabolic dysregulation, with a focus on evaluating the potential involvement of the FASN pathway. These findings may provide a novel experimental foundation for the application of rhubarb-derived natural compounds in pneumonia therapy and identify a potential molecular target for endothelial protection in inflammatory lung disease.

Materials and Methods

Network Pharmacology Analysis

Bioactive components of rhubarb were retrieved from the TCMSP database (https://www.tcmsp-e.com/index.php) using the filtering criteria of oral bioavailability ≥30% and drug-likeness ≥0.18. Their corresponding targets were predicted through TCMSP and SwissTargetPrediction (http://www.swisstargetprediction.ch/) based on SMILES formulas. Pneumonia-related targets were collected from the GeneCards (https://www.genecards.org/), OMIM (https://www.omim.org/), DisGeNET (https://disgenet.com/), and TTD (https://db.idrblab.net/ttd/) databases. Overlapping targets between rhubarb component targets and pneumonia-related targets were visualized using a Venn diagram generated with the venn v1.12 R package. A rhubarb-compound-target-pneumonia network was constructed by importing overlapping targets and active compounds into Cytoscape (version 3.10.1, https://cytoscape.org/), followed by topological property assessment using the "Network Analyzer" function.

Cell Culture and Treatment

HPMVECs (CP-H001, Procell, Wuhan, China) were cultured in HPMVEC complete medium (CM-H001, Procell, Wuhan, China) (37 °C, 5% CO_2) in an incubator. The cells were authenticated by short tandem repeat (STR) profiling and tested negative for mycoplasma contamination. Cells were stimulated with 100 ng/mL LPS (HY-D1056, MedChemExpress, Shanghai, China) for 24 h [11]. Aloe emodin (AE, HY-N0189, MedChemExpress, Shanghai, China) was dissolved in dimethyl sulfoxide and added to the medium to achieve final concentrations of 20 µmol/L or 40 µmol/L [12], either alone or in combination with LPS.

A plasmid encoding full-length FASN (NM_004104, **Supplementary Material**) was constructed using the pcDNA3.1 vector by Genepharma (Shanghai, China). The pcDNA3.1 empty vector (C05008, Genepharma, Shanghai, China) served as the negative control (NC). HPMVECs were cultured in six-well plates and transfected with the FASN overexpression plasmid or NC plasmid using lipofectamine reagent (C0533, Beyotime, Shanghai, China). After 48-h of incubation, the cells were collected for subsequent analyses. Transfection efficiency was verified by quantitative real-time PCR (qRT-PCR) and Western blotting.

Cell Viability Assay

HPMVECs (5×10^3/well) seeded in 96-well plates were subjected to a Cell Counting Kit-8 (CCK-8) (40203ES60, YEASEN, Shanghai, China) assay. After exposure to the indicated conditions, cells were incubated with 10 µL of CCK-8 reagent for 2-h at 37 °C. The optical density was then measured (450 nm) using a microplate reader (CMax Plus, Molecular Devices, Shanghai, China).

Terminal Deoxynucleotidyl Transferase dUTP Nick End Labeling (TUNEL)

Apoptotic cells were detected using a commercial detection kit (C1088, Beyotime, Shanghai, China). HPMVECs grown on coverslips were fixed (4% paraformaldehyde; P39200, ACMEC, Shanghai, China) (30 min), permeabilized (0.1% Triton X-100; T88491, ACMEC, Shanghai, China), and stained (TUNEL reaction mixture; 60 min, 37 °C, darkness). Subsequently, cell nuclei were counterstained with DAPI (C1006, Beyotime, Shanghai, China) for 5 min at room temperature in the dark. Following three additional PBS washes, the coverslips were mounted. TUNEL-positive cells were visualized under a fluorescence microscope (Leica DMI6000 B, Leica Microsystems Wetzlar GmbH, Wetzlar, Germany) and quantified as the ratio of TUNEL-positive nuclei to the total number of DAPI-positive nuclei.

Enzyme-Linked Immunosorbent Assay (ELISA)

Interleukin-6 (IL-6) and tumor necrosis factor-alpha (TNF-α) levels in the culture supernatant were quantified using commercial ELISA kits (E-EL-H6156/ E-EL-H0109, Elabscience, Wuhan, China). The absorbance (450 nm) was measured using a microplate reader.

Nile Red Staining

Lipid droplet accumulation was evaluated using Nile red (HY-D0718, MedChemExpress, Shanghai, China). Briefly, treated HPMVECs were fixed with 4% paraformaldehyde and then incubated with the lipid dye for 30 min at room temperature. Nuclei were counterstained

with DAPI (T19827, TargetMol, Shanghai, China). Images were captured using a fluorescence microscope (Leica DMI6000 B, Leica Microsystems Wetzlar GmbH, Wetzlar, Germany) at ×400 magnification with a scale bar of 50 μm.

Measurement of Lipid Parameters

The levels of free fatty acids (FFA), cholesterol, and triglycerides in cell lysates were measured using commercial kits (E-BC-K013-M/ E-BC-K109-M/ E-BC-F033, Elabscience, Wuhan, China). After treatment, HPMVECs were harvested and lysed. Following centrifugation, the clear supernatants were transferred to new tubes. All subsequent procedures were performed strictly according to the reagent kit manuals, and the optical density at the corresponding wavelengths was measured using a microplate reader.

Quantitative Real-Time PCR (qRT-PCR)

HPMVECs were subjected to RNA extraction using Trizol reagent (R21086, Shyuanye, Shanghai, China). The PrimeScript RT Master Mix (MF949, Mei5bio, Beijing, China) was used for reverse transcription to generate cDNA. Real-time PCR amplification was performed using SYBR Green Master Mix (A25743, ThermoFisher, Waltham, MA, USA) on the 7500 real-time PCR System (Applied Biosystems, Foster City, CA, USA). All primer sequences are provided in Table 1. Gene expression levels were determined using the $2^{-\Delta\Delta CT}$ method, with glyceraldehyde-3-phosphate dehydrogenase (GAPDH) as the internal reference.

Table 1. Primers used in this study.

Genes	Primer sequence (5'-3')
SREBF1 (Human)-F	CGGGCCTTGCATTTTCTGAC
SREBF1 (Human)-R	CCCTGAACCCTCAGTCACG
ACLY (Human)-F	GACTTCGGCAGAGGTAGAGC
ACLY (Human)-R	TCAGGAGTGACCCGAGCATA
SCD1 (Human)-F	CTTGCGATATGCTGTGGTGC
SCD1 (Human)-R	CCGGGGGCTAATGTTCTTGT
FASN (Human)-F	AGGCCTCATAGACCTGCTGA
FASN (Human)-R	GGGAGATGAGGGGAGTTCCT
HMGCR (Human)-F	GTTAACTGGAGCCAGGCTGA
HMGCR (Human)-R	GTGAGTTGGAACTGAGGGCA
GAPDH (Human)-F	GTCTCCTCTGACTTCAACAGCG
GAPDH (Human)-R	ACCACCCTGTTGCTGTAGCCAA

Abbreviation: F, Forward; R, Reverse; *SREBF1*, sterol regulatory element binding transcription factor 1; *ACLY*, ATP citrate lyase; *SCD1*, stearoyl-CoA desaturase; *FASN*, Fatty acid synthase; *HMGCR*, 3-hydroxy-3-methylglutaryl-CoA reductase.

Molecular Docking

The 3D crystal structure of FASN was downloaded from the Protein Data Bank (https://www.rcsb.org/, PDB ID: 8VF7), while the molecular configuration of AE was obtained from the PubChem database (https://pubchem.ncbi.nlm.nih.gov/) using its SMILES formula: C1=CC2=C(C(=C1)O)C(=O)C3=C(C2=O)C=C(C=C3O)CO. Hydrogenation and dehydration treatments were performed using AutoDockTools 1.5.7 software (The Scripps Research Institute, La Jolla, CA, USA). The docking grid box was centered at coordinates (center_x = 192.4, center_y = 220.473, center_z = 187.245) with dimensions of size_x = 94, size_y = 108, and size_z = 126, covering the entire putative binding pocket of FASN. After defining the parameters of the active pocket, molecular docking was performed using SailVina 1.0 software (SailVina, https://github.com/sailvina). The binding activity between AE and FASN was evaluated based on binding energy, with a screening criterion of binding energy ≤–5 kcal/mol. Finally, the docking conformations were visualized using PyMol 2.3.4 software (Schrödinger, LLC, New York, NY, USA).

Western Blot

Protein lysates were extracted from HPMVECs using RIPA Lysis Buffer (AP01L013, Life-iLab, Shanghai, China). Equal amounts of protein (20 μg) were loaded for SDS-PAGE (190916-40, YaJi Biological, Shanghai, China) and transferred onto PVDF membranes (WJ001S, epizyme, Shanghai, China). The membranes were blocked with specialized buffer (AP36L118, Life-iLab, Shanghai, China), followed by incubation with primary antibodies (Table 2) (4 °C overnight), washing, and incubation with HRP-linked secondary antibodies (Table 2). Protein bands were visualized using an ECL kit (YWB003, YFXBIO, Nanjing, China), and signals were documented with a SynGene imaging system (G:BOX F3, Cambridge, UK).

Table 2. Antibodies used in this study.

Name	Catalog	Dilution	Manufacturer
FASN	ab128870	1/10,000	Abcam
GAPDH	ab8245	1/10,000	Abcam
goat anti rabbit	ab205718	1/10,000	Abcam
goat anti mouse	ab205719	1/10,000	Abcam

Statistical Analysis

All experiments were performed at least three times. Data normality was assessed using the Shapiro-Wilk test. Differences between groups were analyzed using Student's *t*-test (two groups) or one-way analysis of variance (ANOVA) followed by Tukey's post hoc test (multiple groups). Experimental data were analyzed using SPSS 21.0 software (SPSS Inc., Chicago, IL, USA) and presented as Mean ± SD, with statistical significance set at $p < 0.05$.

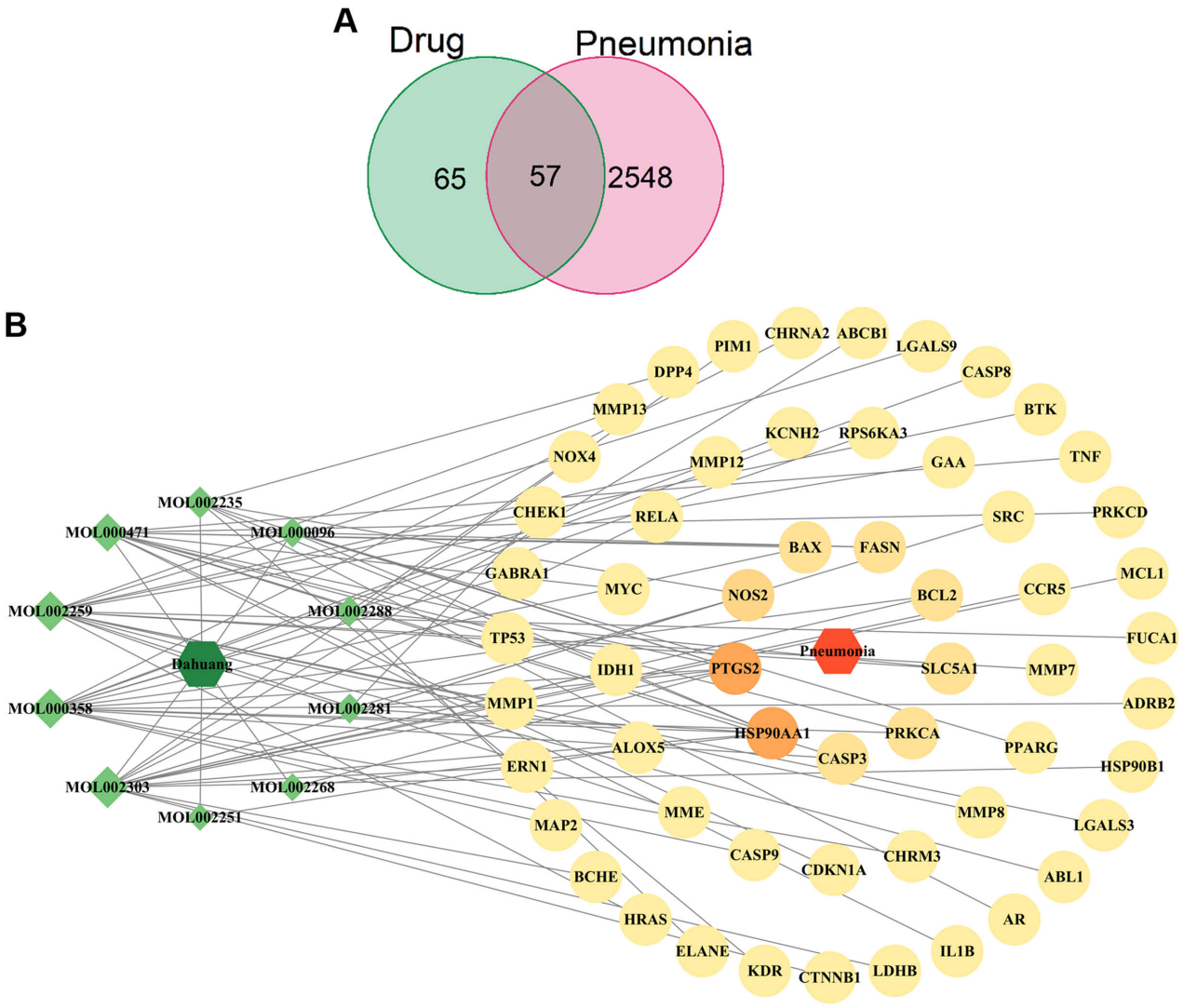


Fig. 1. Network pharmacology screening of potential targets for rhubarb in pneumonia treatment. (A) Venn diagram showing the overlap between rhubarb component targets and pneumonia-related targets. (B) Component-target-pneumonia interaction network.

Results

Network Pharmacology Prediction of Rhubarb Components Targeting Pneumonia

A total of 122 targets of rhubarb bioactive components were identified. Among these, 57 targets overlapped with known pneumonia-related disease targets (Fig. 1A). A component-target-pneumonia interaction network was constructed (Fig. 1B).

AE Attenuates LPS-Induced Cellular Injury, Inflammation, and Lipid Droplet Accumulation in HPMVECs

To verify the protective effect of AE, *in vitro* assays were conducted in LPS-stimulated HPMVECs. Cell viability of HPMVECs was significantly reduced following LPS stimulation, whereas this reduction was partially reversed by AE treatment (Fig. 2A, $p < 0.01$). A notable increase in TUNEL positive cells was observed after LPS stimulation, which was dose-dependently attenuated by AE treatment (Fig. 2B,E, $p < 0.001$). Meanwhile, LPS exposure substantially upregulated the inflammatory mediators IL-6 and TNF-α, and both cytokines were dose-dependently downregulated by AE (Fig. 2C,D, $p < 0.01$). LPS-induced lipid droplet accumulation was also alleviated by AE treatment (Fig. 3A,B, $p < 0.05$). Collectively, AE protects HPMVECs against LPS-induced injury, inflammation, and abnormal lipid deposition.

AE Improves LPS-Induced Lipid Metabolism Disorder in HPMVECs

The effect of AE on lipid metabolism was further investigated. LPS stimulation significantly increased cholesterol and triglyceride levels, whereas it reduced FFA levels (Fig. 4A–C, $p < 0.001$). AE treatment reversed these changes in a dose-dependent manner (Fig. 4A–C, $p < 0.05$).

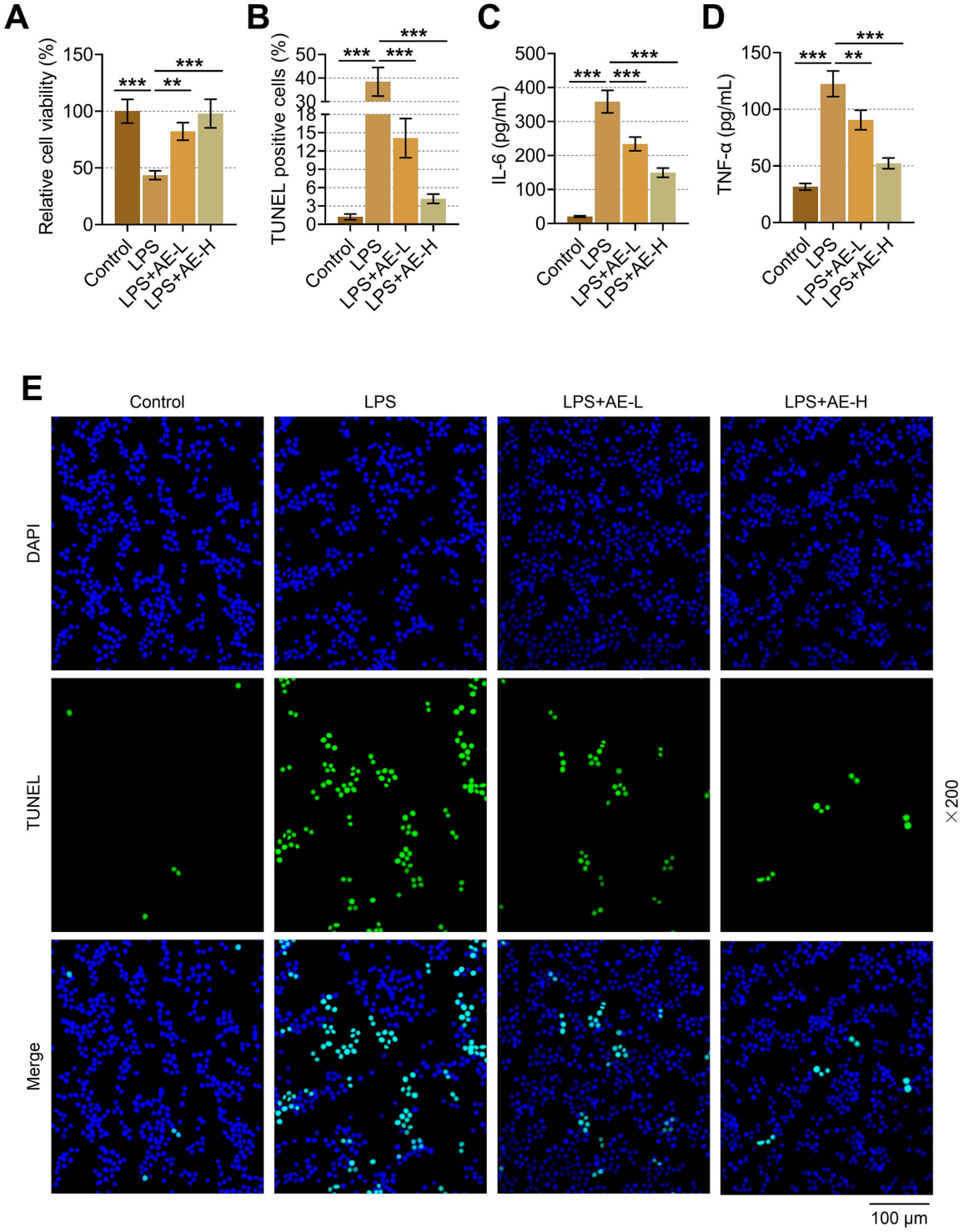


Fig. 2. AE protects against LPS-induced cell injury and inflammation *in vitro*. HPMVECs were stimulated with 100 ng/mL LPS (24 h), with/without AE (20/40 μmol/L). (A) Cell viability (Cell Counting Kit 8 (CCK-8) assay). (B,E) TUNEL positive cells (TUNEL staining; ×200, scale bar: 100 μm). (C,D) Quantification of pro-inflammatory cytokines IL-6 and TNF-α (ELISA). Data are mean ± SD (n = 3). $^{**}p < 0.01$, $^{***}p < 0.001$. AE, Aloe emodin; LPS, lipopolysaccharide; IL-6, interleukin-6; TNF-α, tumor necrosis factor-alpha; TUNEL, terminal deoxynucleotidyl transferase dUTP nick end labeling.

The mRNA expression of key lipogenic genes, including SREBF1, ACLY, SCD1, FASN, and HMGCR, was significantly upregulated in the LPS group (Fig. 4D–H, $p < 0.001$). AE treatment notably downregulated the mRNA expression of these genes (Fig. 4D–H, $p < 0.05$). These data suggest that AE ameliorates LPS-induced dysregulation of

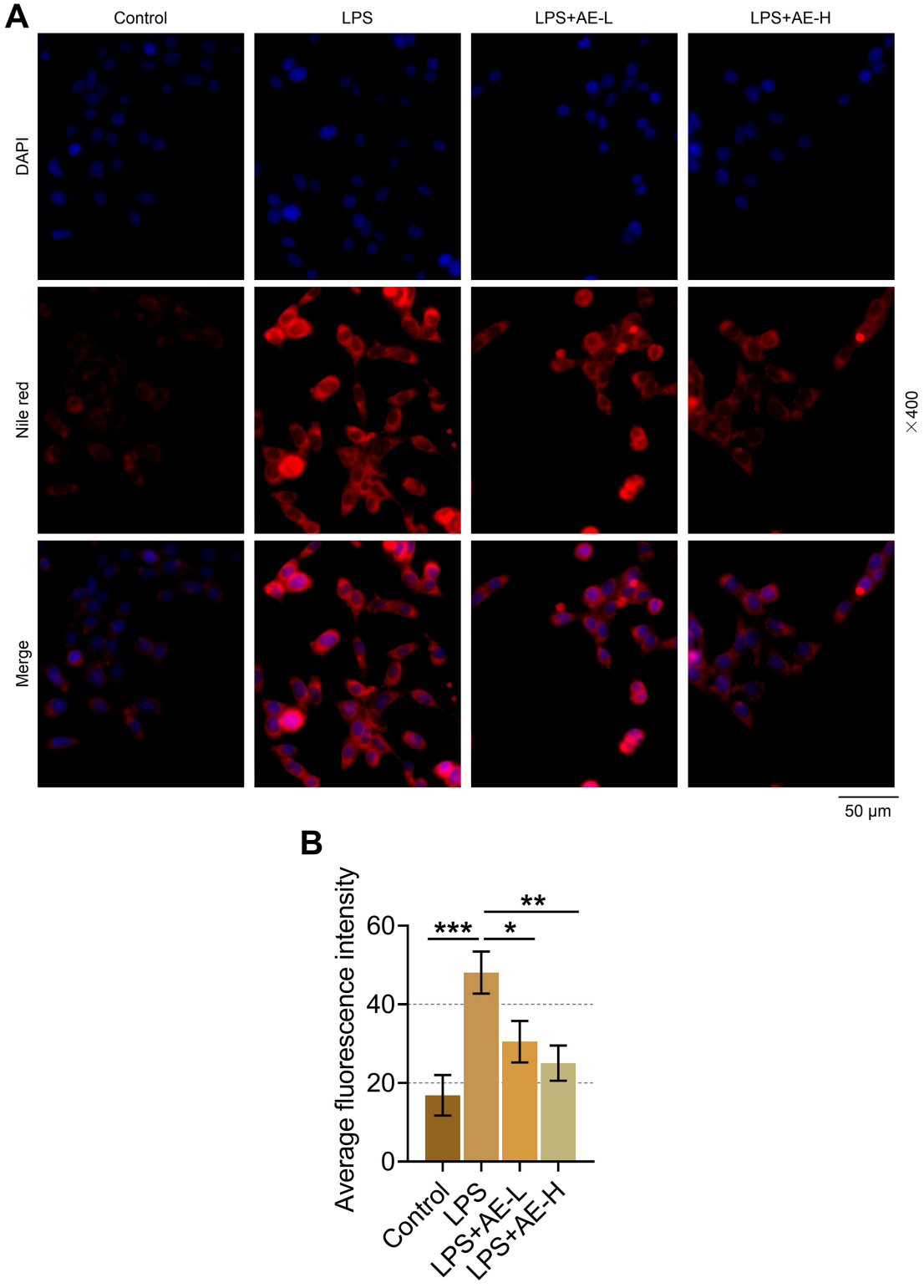


Fig. 3. AE protects against LPS-induced lipid droplet accumulation *in vitro*. HPMVECs were stimulated with 100 ng/mL LPS (24 h), with/without AE (20/40 μmol/L). (A,B) Lipid droplet accumulation (Nile Red staining; ×400, scale bar: 50 μm). Data are mean ± SD (n = 3). $^{*}p < 0.05$, $^{**}p < 0.01$, $^{***}p < 0.001$.

lipid metabolism in HPMVECs. In addition, based on these experimental results, 40 μmol/L AE demonstrated superior protective effects on cell viability, anti-inflammatory properties, and lipid metabolism restoration compared with 20 μmol/L AE. Therefore, 40 μmol/L AE was selected for subsequent mechanistic experiments.

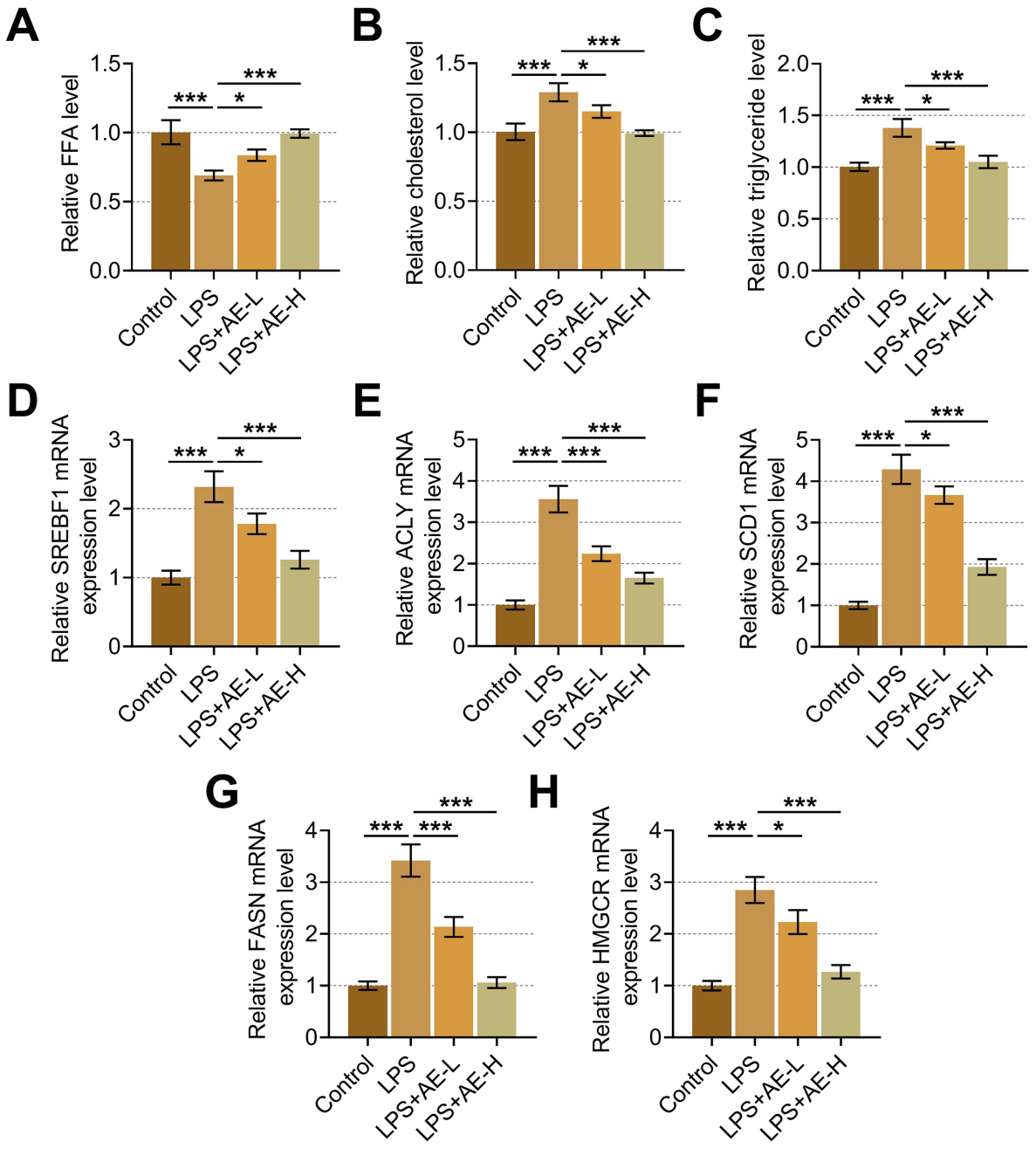


Fig. 4. AE ameliorates LPS-induced lipid metabolism disorder in HPMVECs. HPMVECs were stimulated with 100 ng/mL LPS (24 h), with/without AE (20/40 µmol/L). (A–C) Relative levels of free fatty acids (FFA), cholesterol, and triglycerides (commercial kits). (D–H) The mRNA expression levels of lipid metabolism-related genes *SREBF1*, *ACLY*, *SCD1*, *FASN*, and *HMGCR* (qRT-PCR). Data are mean ± SD (n = 3). $^{*}p < 0.05$, $^{***}p < 0.001$. qRT-PCR, quantitative real-time PCR; SREBF1, sterol regulatory element binding transcription factor 1; ACLY, ATP citrate lyase; SCD1, stearoyl-CoA desaturase; FASN, Fatty acid synthase; HMGCR, 3-hydroxy-3-methylglutaryl-CoA reductase.

Molecular Docking Prediction and Functional Assessment of FASN Involvement

To identify the potential target of AE, molecular docking was performed. The simulation showed that AE formed stable hydrogen bonds with key residues of FASN (Fig. 5A), and the binding energy between AE and FASN was –8.0 kcal/mol. This computational prediction suggests a potential interaction between AE and FASN. A FASN overexpression plasmid was transfected into HPMVECs. Both FASN mRNA and protein levels were significantly elevated in the FASN overexpression group (Fig. 5B–D, $p < 0.001$).

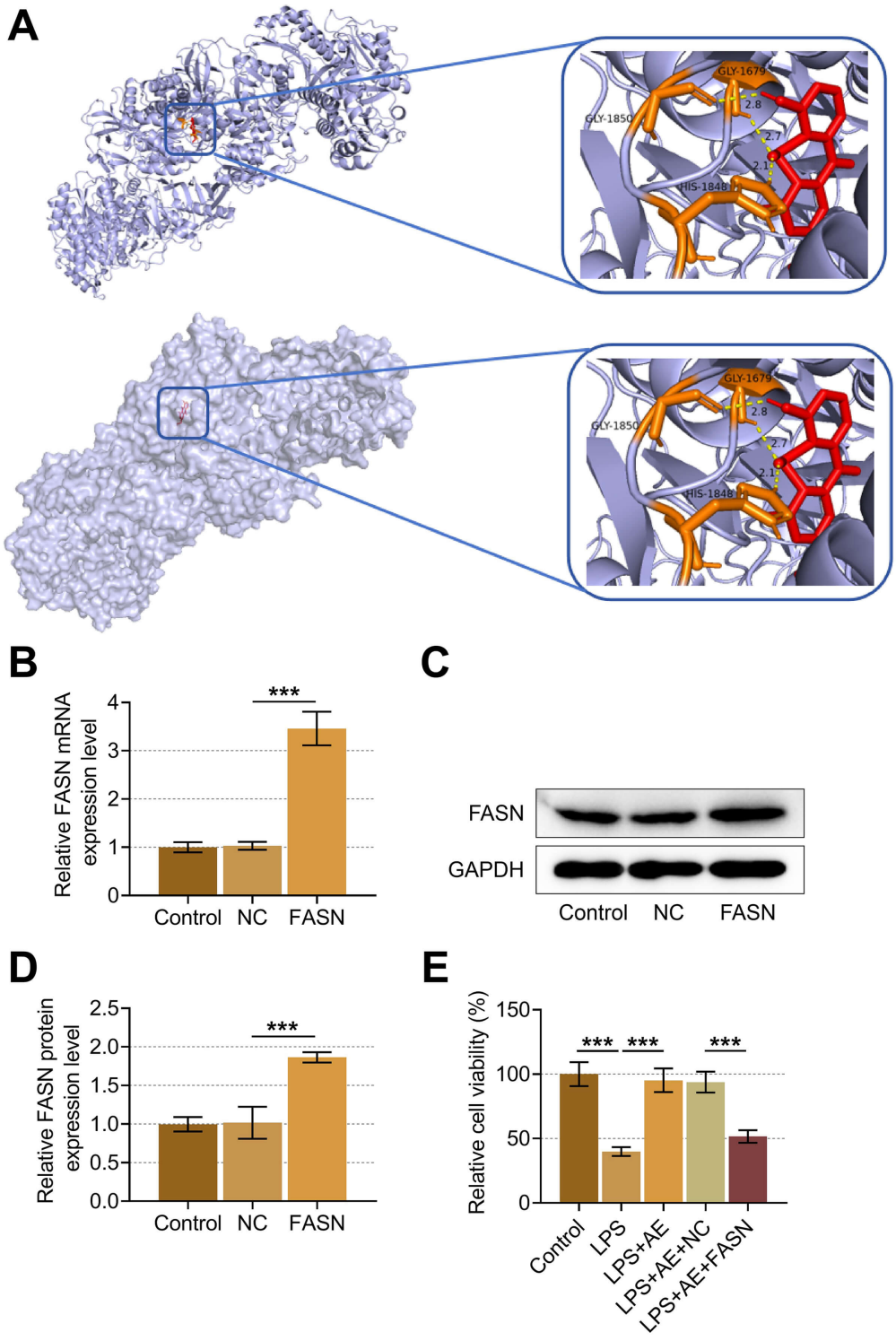


Fig. 5. Molecular docking and functional verification of AE targeting FASN. (A) Molecular docking of AE and FASN. (B–D) FASN overexpression efficiency (qRT-PCR and Western blotting). (E) Cell viability (CCK-8 assay). Data are mean ± SD (n = 3). ***$p < 0.001$.

FASN Overexpression Attenuates the Protective Effects of AE in LPS-stimulated HPMVECs

To establish whether FASN mediates the cytoprotective effects of AE, rescue experiments were performed. FASN overexpression attenuated the ability of AE to preserve cell viability under LPS challenge (Fig. 5E, $p < 0.001$). The inhibitory effect of AE on TUNEL-positive cells was significantly weakened by FASN overexpression (Fig. 6A,D, $p < 0.001$). Similarly, the inhibitory effects of AE on IL-6 and TNF-α levels were weakened in the FASN

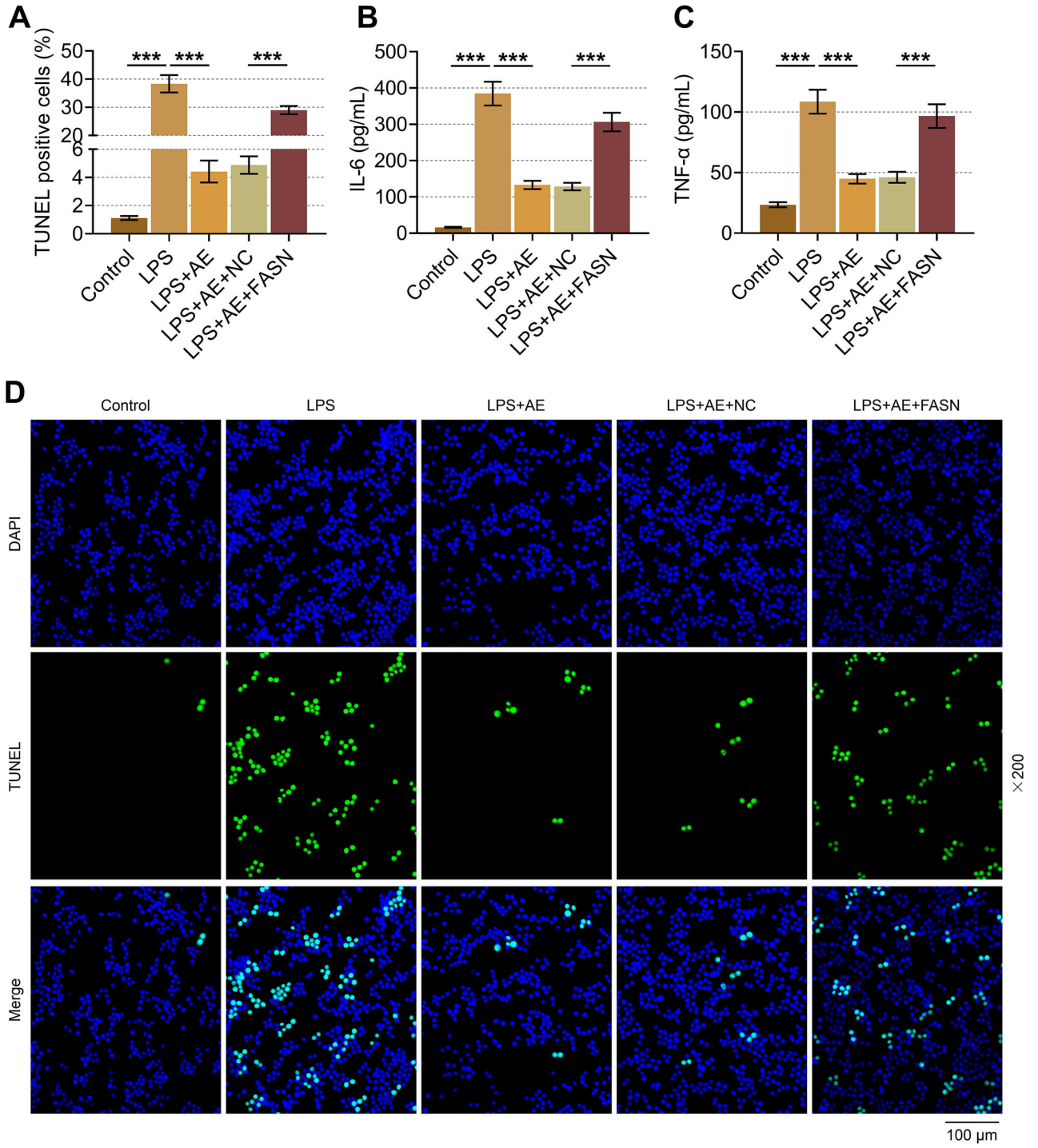


Fig. 6. FASN overexpression weakens the protective effects of AE against LPS-induced injury in HPMVECs. HPMVECs were transfected with FASN or NC plasmid, then treated with LPS (100 ng/mL) and/or AE (40 μmol/L). (A,D) TUNEL positive cells (TUNEL staining; ×200, scale bar: 100 μm). (B,C) Levels of pro-inflammatory cytokines IL-6 and TNF-α (ELISA). Data are mean ± SD (n = 3). $^{***}p < 0.001$.

overexpression group (Fig. 6B,C, $p < 0.001$). Additionally, the reduction in lipid droplet accumulation mediated by AE was also weakened by FASN overexpression (Fig. 7A,B, $p < 0.01$).

FASN overexpression weakened the effects of AE on lipid parameters. Specifically, the AE-induced increase in FFA levels was abolished, and the AE-mediated reductions in cholesterol and triglycerides were largely reversed (Fig. 8A–C, $p < 0.05$). Consistently, the AE-induced downregu-

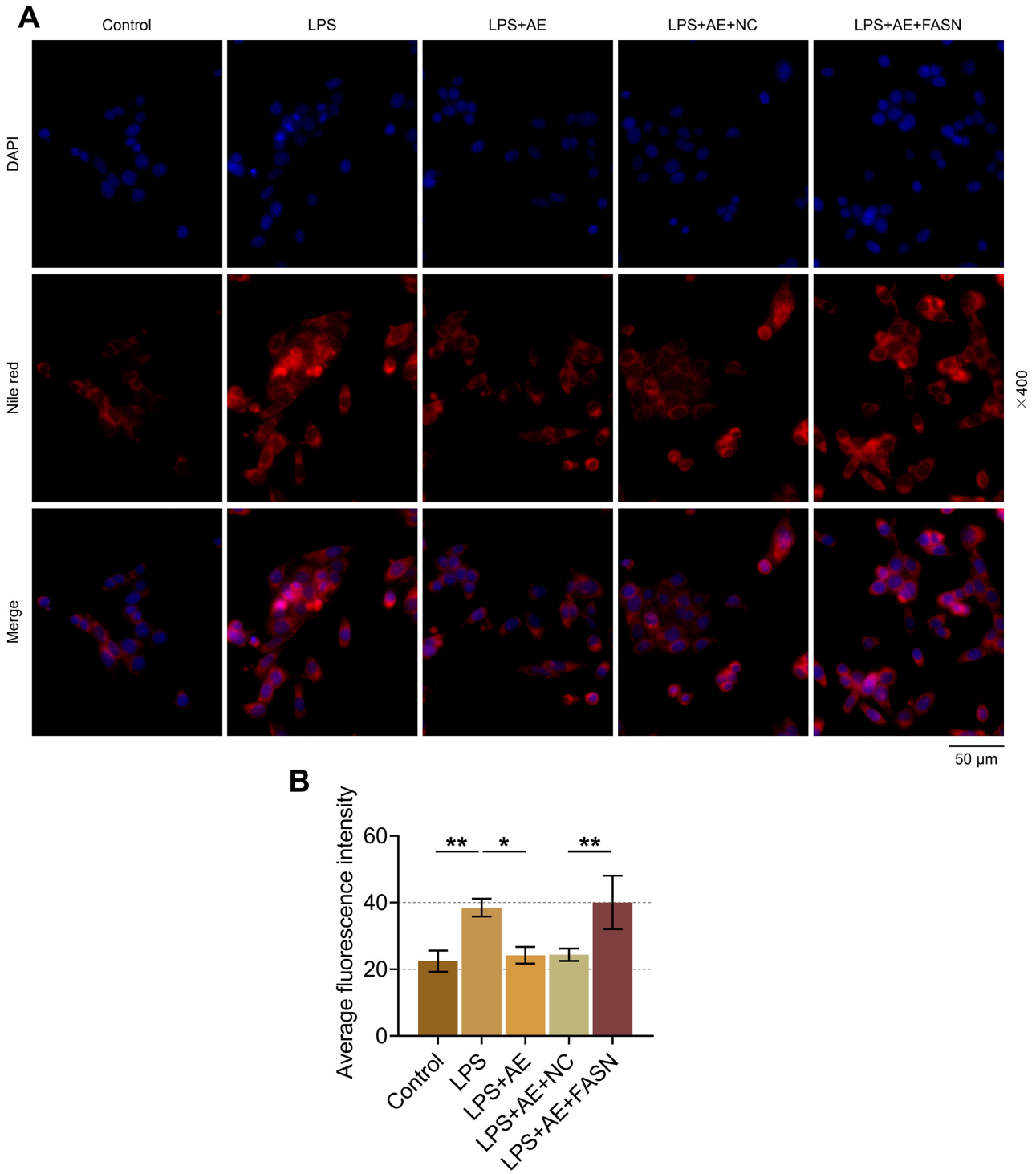


Fig. 7. FASN overexpression weakens the effects of AE on lipid droplet accumulation in LPS-induced HPMVECs. (A,B) Lipid droplet accumulation (Nile Red staining; ×400, scale bar: 50 μm). Data are mean ± SD (n = 3). $^{*}p < 0.05$, $^{**}p < 0.01$.

lation of lipid metabolism-related genes mRNA expression, including SREBF1, ACLY, SCD1, FASN, and HMGCR, was notably abolished by FASN overexpression (Fig. 8D–H, $p < 0.01$).

Discussion

In this study, we combined network pharmacology prediction with *in vitro* functional assays to investigate the protective effects of AE on LPS-stimulated HPMVECs. Our results indicate that AE alleviates LPS-induced injury and that FASN may be involved in mediating these protec-

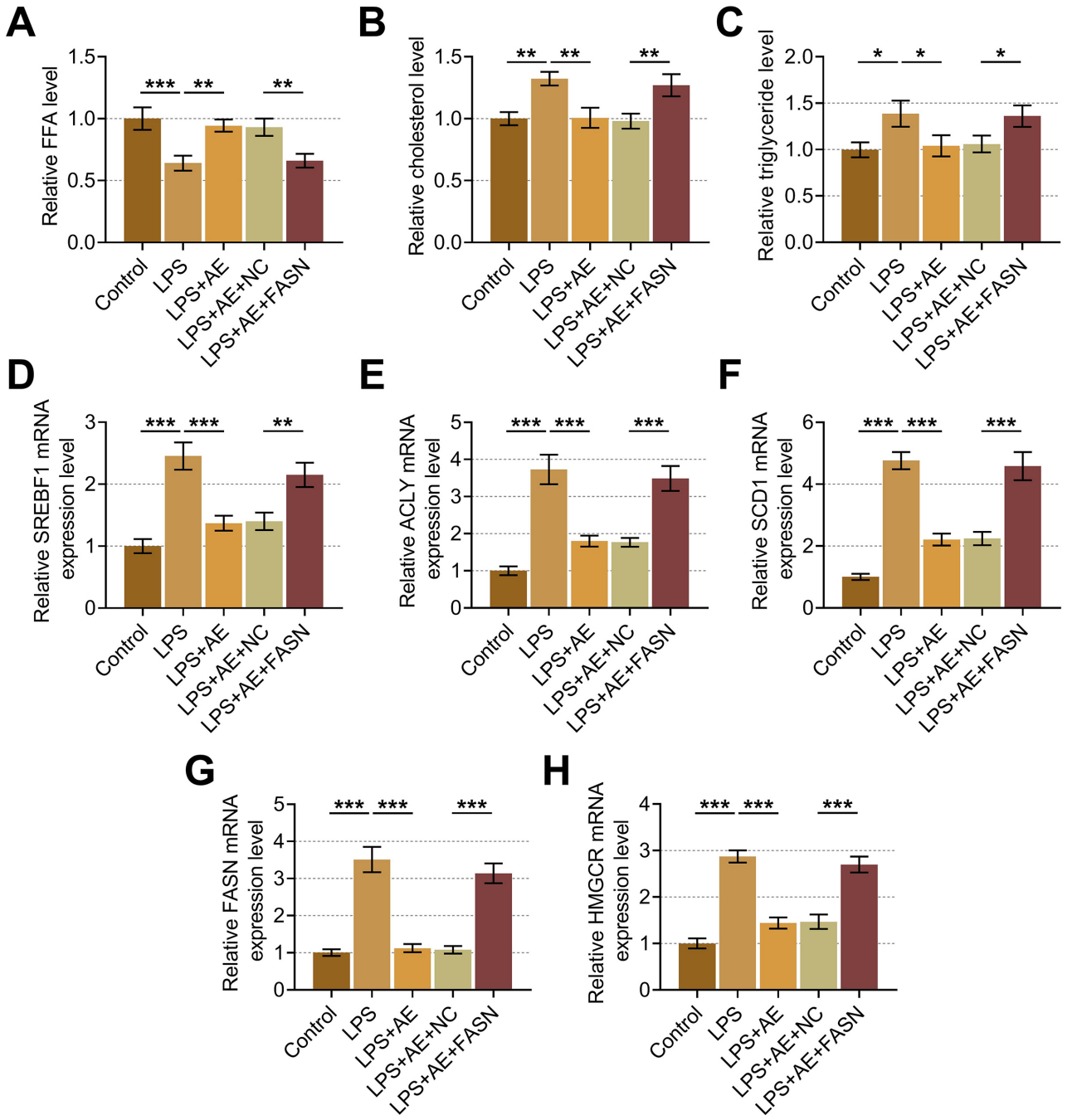


Fig. 8. FASN overexpression weakens the regulatory effects of AE on lipid metabolism in LPS-stimulated HPMVECs. HPMVECs were transfected with FASN or NC plasmid, then treated with LPS (100 ng/mL) and/or AE (40 μmol/L). (A–C) Relative levels of FFA, cholesterol, and triglycerides (commercial kits). (D–H) The mRNA expression levels of lipid metabolism-related genes *SREBF1*, *ACLY*, *SCD1*, *FASN*, and *HMGCR* (qRT-PCR). Data are mean ± SD (n = 3). $^{*}p < 0.05$, $^{**}p < 0.01$, $^{***}p < 0.001$.

tive effects. These findings provide a preliminary experimental basis for the potential application of rhubarb-derived anthraquinones in protecting the pulmonary endothelium.

Pulmonary microvascular endothelial barrier dysfunction is recognized as a central pathological event in pneumonia, in which excessive endothelial apoptosis directly contributes to increased vascular permeability and pulmonary edema [13,14]. In the present study, a marked reduction in LPS-induced HPMVEC apoptosis was observed following AE treatment, consistent with previous findings showing that emodin, a congener anthraquinone of AE, alleviated ALI by suppressing ferroptosis and improving mitochondrial function in LPS-challenged vascular endothelial cells [15]. Moreover, the release of inflammatory

cytokines is known to further disrupt endothelial barrier integrity. Pro-inflammatory mediators can downregulate tight junction proteins, impair endothelial adhesion, and aggravate vascular leakage [16]. In this study, LPS stimulation significantly upregulated IL-6 and TNF-α levels in HPMVECs, and both cytokines were suppressed by AE in a concentration-dependent manner. This anti-inflammatory property is consistent with the well-recognized activity of rhubarb-derived anthraquinones, including AE [17]. Network pharmacology analyses have also suggested that these compounds ameliorate ALI through the regulation of inflammatory and oxidative damage pathways [18,19]. Lipid metabolism disturbance is another important driver of endothelial barrier dysfunction. Abnormal accumulation of cholesterol and triglycerides can induce endoplasmic reticulum stress and reactive oxygen species bursts, thereby damaging endothelial membrane integrity. Conversely, excessive reductions in FFA levels may impair mitochondrial β-oxidation, leading to energy deficiency and compromised barrier repair capacity. In the current study, AE treatment significantly attenuated LPS-induced lipid droplet accumulation and reversed metabolic alterations characterized by elevated cholesterol and triglycerides along with reduced FFA levels [20]. Similar protective effects have been reported by Li et al. [21], who demonstrated that AE reduced intracellular lipid accumulation and suppressed lipogenic gene expression in FFA-stimulated hepatocytes, thereby ameliorating non-alcoholic fatty liver disease. Collectively, these multi-dimensional and coordinated actions of AE on inflammation, apoptosis, and lipid metabolism suggest a more comprehensive endothelial protective advantage compared with single-target agents.

At the mechanistic level, the core contribution of this study is the identification of FASN as a potential mediator of AE-mediated anti-inflammatory and anti-lipogenic effects. Molecular docking in the current study predicted a potential binding mode between AE and FASN, a finding consistent with a previous report in which network pharmacology combined with bioinformatics predicted a stable AE-FASN complex and suggested FASN as a potential candidate target of AE in hepatocellular carcinoma [22]. FASN is a pivotal rate-limiting enzyme responsible for the terminal step of de novo fatty acid synthesis, and its involvement in ALI/ARDS pathogenesis has gained increasing attention in recent years. In a study by Wu and colleagues, FASN protein levels were found to be significantly upregulated in pulmonary endothelial cells of obese mice following LPS challenge. Inhibition of FASN, either by the chemical inhibitor C75 or by shRNA, substantially reduced the overproduction of pulmonary inflammatory cytokines, alleviated vascular hyperpermeability, and preserved endothelial barrier function through upregulation of VE-cadherin expression [6]. Based on these observations, it is inferred that FASN serves not only as a critical risk factor for endothelial injury in pneumonia but also as a potential functional target through which AE exerts its multifaceted endothelial protective effects. Furthermore, the regulatory effect of AE on lipid metabolism is not confined to FASN alone. It has been demonstrated that Danzhi Tiaozhi Decoction, a formulation containing AE, significantly suppressed the expression of SREBP1c and FAS (the protein encoded by FASN) and improved lipid metabolic disorders [23]. Hence, the modulatory influence of AE on FASN may involve a cascade relationship with upstream transcriptional regulators such as SREBP1c. This dual mechanism, combining computationally predicted binding with indirect transcriptional regulation, provides a molecular basis for the protective effects of AE against LPS-induced endothelial lipid dysregulation.

Several limitations should be recognized in this work. First, although molecular docking predicted the binding interface between AE and FASN, and prior evidence indicates that emodin promotes FASN degradation via the ubiquitin-proteasome system [24], whether AE regulates FASN protein stability through a similar mechanism remains to be clarified. Direct pharmacological intervention using FASN-specific enzyme activity inhibitors and measurement of protein half-life are required for further validation. Second, while the LPS-treated HPMVEC model provides a standardized setting, it incompletely recapitulates the multiple cell types and interactions present in an intact organism. Therefore, future studies should employ animal models to validate whether AE targets FASN and exerts therapeutic effects in pneumonia. Third, the rescue experiments lacked an LPS + FASN overexpression-alone group and FASN knockdown validation. Consequently, we cannot exclude the possibility that FASN overexpression itself may exacerbate LPS-induced damage, nor can we establish a complete causal relationship. Therefore, our findings are limited to demonstrating that FASN overexpression can attenuate the protective phenotype conferred by AE.

Conclusion

Taken together, the present work provides initial evidence that AE confers against LPS-induced apoptosis, inflammation, and lipid metabolic dysregulation in HPMVECs, with FASN identified as a potential mediator of these effects. The restoration of lipid metabolic homeostasis and suppression of pro-inflammatory and pro-apoptotic signals together constitute a refined network regulatory mechanism. The current observations provide a novel experimental rationale for further exploring rhubarb-derived anthraquinones as candidates to alleviate LPS-induced endothelial cell damage, while also revealing a candidate molecular target for future investigation.

Availability of Data and Materials

The datasets used or analyzed during the current study are available from the corresponding authors upon reasonable request.

Author Contributions

SPZ: Conceptualization, Methodology, Formal analysis, Writing- original draft, Writing -review & editing; HRD: Data duration, Formal analysis, Investigation, Writing- original draft, Writing - review & editing; XCD: Data curation, Visualization, Investigation, Writing - original draft, Writing - review & editing; LHZ: Conceptualization, Methodology, Validation, Writing - original draft, Writing - review & editing; ZJL: Conceptualization, Investigation, Formal analysis, Writing- original draft, Writing - review & editing. All authors gave final approval of the version to be published. All authors have participated sufficiently in the work to take public responsibility for appropriate portions of the content and agreed to be accountable for all aspects of the work in ensuring that questions related to its accuracy or integrity.

Ethics Approval and Consent to Participate

Not applicable.

Acknowledgment

Not applicable.

Funding

This work was supported by Zhejiang Provincial Administration of Traditional Chinese Medicine (Zhejiang Provincial Traditional Chinese Medicine Science and Technology Program Project) [grant number: 2024ZR128].

Conflict of Interest

The authors declare no conflict of interest.

Supplementary Material

Supplementary material associated with this article can be found, in the online version, at https://doi.org/10.24976/Discov.Med.202638214.267.

References

[1] Zhang J, Guo Y, Mak M, Tao Z. Translational medicine for acute lung injury. Journal of Translational Medicine. 2024; 22: 25. https://doi.org/10.1186/s12967-023-04828-7

[2] Barkat MQ, Li Q, Manzoor M, Xu C, Hussain N, Salawi A, et al. Sepsis-induced ALI/ARDS beyond supportive care: molecular mechanisms and cutting-edge therapies. International Immunopharmacology. 2025; 166: 115495. https://doi.org/10.1016/j.intimp.2025.115495

[3] Zeng Y, Fu BM. Angiogenesis and Microvascular Permeability. Cold Spring Harbor Perspectives in Medicine. 2025; 15: a041163. https://doi.org/10.1101/cshperspect.a041163

[4] Lu X, Li G, Liu Y, Luo G, Ding S, Zhang T, et al. The role of fatty acid metabolism in acute lung injury: a special focus on immunometabolism. Cellular and Molecular Life Sciences : CMLS. 2024; 81: 120. https://doi.org/10.1007/s00018-024-05131-4

[5] Yoon H, Shaw JL, Haigis MC, Greka A. Lipid metabolism in sickness and in health: Emerging regulators of lipotoxicity. Molecular Cell. 2021; 81: 3708–3730. https://doi.org/10.1016/j.molcel.2021.08.027

[6] Wu Z, Zhu L, Nie X, Liu Y, Zhang X, Qi Y. Inhibition of fatty acid synthase protects obese mice from acute lung injury via ameliorating lung endothelial dysfunction. Respiratory Research. 2023; 24: 81. https://doi.org/10.1186/s12931-023-02382-w

[7] Qiu J, Xu F, Wei H, Gao Y, Liu N, Zhao J, et al. Metabolic restoration: Rhubarb polysaccharides as a shield against non-alcoholic fatty liver disease. International Journal of Biological Macromolecules. 2025; 305: 141151. https://doi.org/10.1016/j.ijbiomac.2025.141151

[8] Régnier M, Rastelli M, Morissette A, Suriano F, Le Roy T, Pilon G, et al. Rhubarb Supplementation Prevents Diet-Induced Obesity and Diabetes in Association with Increased *Akkermansia muciniphila* in Mice. Nutrients. 2020; 12: 2932. https://doi.org/10.3390/nu12102932

[9] Annie SA, Khan MA, Talukder A, Alam AK, Uddin MJ. Unraveling the Therapeutic Mechanisms of Aloe-Emodin: A Natural Anthraquinone With Promising Health Benefits. Archiv Der Pharmazie. 2026; 359: e70247. https://doi.org/10.1002/ardp.70247

[10] Xie J, Zhang J, Chen X. Aloe-emodin: from pharmacological mechanisms to clinical applications and future perspectives. Frontiers in Pharmacology. 2026; 16: 1741679. https://doi.org/10.3389/fphar.2025.1741679

[11] Yang J, Ruan F, Zheng Z. Ripasudil Attenuates Lipopolysaccharide (LPS)-Mediated Apoptosis and Inflammation in Pulmonary Microvascular Endothelial Cells via ROCK2/eNOS Signaling. Medical Science Monitor : International Medical Journal of Experimental and Clinical Research. 2018; 24: 3212–3219. https://doi.org/10.12659/MSM.910184

[12] Bao W, Lyu J, Feng G, Guo L, Zhao D, You K, et al. Aloe emodin promotes mucosal healing by modifying the differentiation fate of enteroendocrine cells *via* regulating cellular free fatty acid sensitivity. Acta Pharmaceutica Sinica. B. 2024; 14: 3964–3982. https://doi.org/10.1016/j.apsb.2024.05.027

[13] Fu H, Gao B, Zhou X, Hao Y, Liu C, Lan A, et al. DNA dioxygenase TET2 deficiency aggravates sepsis-induced acute lung injury by targeting ITGA10 via the PI3K/AKT signaling pathway. Cellular & Molecular Biology Letters. 2025; 30: 60. https://doi.org/10.1186/s11658-025-00739-1

[14] Joffre J, Hellman J, Ince C, Ait-Oufella H. Endothelial Responses in Sepsis. American Journal of Respiratory and Critical Care Medicine. 2020; 202: 361–370. https://doi.org/10.1164/rccm.201910-1911TR

[15] Li J, Wang Y, Zhang C, Li S, Qi W. Emodin Alleviates Microcirculation Disorders in Acute Lung Injury Associated With Severe Acute Pancreatitis by Inhibiting Ferroptosis of Vascular Endothelial Cells. Pancreas. 2026; 55: e856–e867. https://doi.org/10.1097/MPA.0000000000002666

[16] Tang F, Zhao XL, Xu LY, Zhang JN, Ao H, Peng C. Endothelial dysfunction: Pathophysiology and therapeutic targets for sepsis-induced multiple organ dysfunction syndrome. Biomedicine & Pharmacotherapy = Biomedecine & Pharmacotherapie. 2024; 178: 117180. https://doi.org/10.1016/j.biopha.2024.117180

[17] Wang D, Wang XH, Yu X, Cao F, Cai X, Chen P, et al. Pharmacokinetics of Anthraquinones from Medicinal Plants. Frontiers in Pharmacology. 2021; 12: 638993. https://doi.org/10.3389/fphar.2021.638993

[18] Wang Y, Jin X, Fan Q, Li C, Zhang M, Wang Y, et al. Deciphering the Active Compounds and Mechanisms of HSBDF for

Treating ALI *via* Integrating Chemical Bioinformatics Analysis. Frontiers in Pharmacology. 2022; 13: 879268. https://doi.org/10.3389/fphar.2022.879268

[19] Luo C, Ye YH, Jiang C, Ning B, Ke J, Chen G. Mechanism of Xuanbai Chengqi Decoction in treating acute lung injury based on network pharmacology and experimental verification. Zhongguo Zhong Yao Za Zhi. 2024; 49: 4329–4337. https://doi.org/10.19540/j.cnki.cjcmm.20240513.702 (In Chinese)

[20] Mallick R, Duttaroy AK. Modulation of endothelium function by fatty acids. Molecular and Cellular Biochemistry. 2022; 477: 15–38. https://doi.org/10.1007/s11010-021-04260-9

[21] Li W, Pan M, Tang J. Aloe-emodin ameliorates non-alcoholic fatty liver disease by regulating the ZNRF3/Wnt/β-catenin axis and suppressing hepatic lipogenesis. Biochemical and Biophysical Research Communications. 2026; 827: 153979. https://doi.org/10.1016/j.bbrc.2026.153979

[22] Wei J, Chen H, Xu M, Zhang Z, Wang J, Jiang W, et al. Prediction of potential targets of aloe-emodin in the treatment of hepatocellular carcinoma using network pharmacology combined with bioinformatics. Discover Oncology. 2025; 16: 464. https://doi.org/10.1007/s12672-025-02215-w

[23] Jiang X, Tang N, Liu Y, Wang Z, Chen J, Liu F, et al. Integrating network analysis and pharmacokinetics to investigate the mechanisms of Danzhi Tiaozhi Decoction in metabolic-associated fatty liver disease (MAFLD). Journal of Ethnopharmacology. 2024; 318: 117008. https://doi.org/10.1016/j.jep.2023.117008

[24] Lee KH, Lee MS, Cha EY, Sul JY, Lee JS, Kim JS, et al. Inhibitory effect of emodin on fatty acid synthase, colon cancer proliferation and apoptosis. Molecular Medicine Reports. 2017; 15: 2163–2173. https://doi.org/10.3892/mmr.2017.6254